



Geophysical Research Letters

RESEARCH LETTER

10.1029/2018GL078455

Key Points:

- We conducted CMT inversions of shallow very low frequency earthquakes using a 3-D velocity structure model and onshore seismic network
- A suitable 3-D velocity structure model enables us to obtain accurate CMT solutions of events before seafloor observations
- Our CMT solutions suggest seismic slip around the very shallow part of the plate boundary beneath the accretionary prism toe

Supporting Information:

- Supporting Information S1
- Data Set S1
- Data Set S2
- Data Set S3

Correspondence to:

S. Takemura,
shunsuke@bosai.go.jp

Citation:

Takemura, S., Matsuzawa, T., Kimura, T., Tonegawa, T., & Shiomi, K. (2018).

Centroid moment tensor inversion of shallow very low frequency earthquakes off the Kii Peninsula, Japan, using a three-dimensional velocity structure model. *Geophysical Research Letters*, 45. <https://doi.org/10.1029/2018GL078455>

Received 24 APR 2018

Accepted 19 JUN 2018

Accepted article online 26 JUN 2018

Centroid Moment Tensor Inversion of Shallow Very Low Frequency Earthquakes Off the Kii Peninsula, Japan, Using a Three-Dimensional Velocity Structure Model

Shunsuke Takemura¹ , Takanori Matsuzawa¹ , Takeshi Kimura¹ , Takashi Tonegawa² , and Katsuhiko Shiomi¹ 

¹National Research Institute for Earth Science and Disaster Resilience, Tsukuba, Japan, ²Japan Agency for Marine-Earth Science and Technology, Yokohama, Japan

Abstract We conducted centroid moment tensor inversions of shallow very low frequency earthquakes (SVLFEs) that occurred around off the southeast Kii Peninsula, Japan. A set of Green's functions was evaluated using numerical simulations of seismic wave propagation in a three-dimensional velocity structure model, including the subducting Philippine Sea slab and the accretionary prism. We used observed seismograms for periods of 20–50 s at an onshore broadband network, which enable us to investigate the long-term activity of SVLFEs. Estimated centroid locations and focal mechanisms of SVLFEs, including SVLFEs that occurred prior to the deployment of seafloor observations, were very similar to those estimated using seafloor records. Low-angle thrust faulting mechanisms were concentrated around the accretionary prism toe. SVLFE activity in April 2016 was concentrated further west in an area of previous activity. Our results imply seismic slip around the very shallow part of the Philippine Sea plate boundary.

Plain Language Summary We investigated locations and focal mechanisms of shallow very low frequency earthquakes (SVLFEs) that occurred off the southeast Kii Peninsula, Japan, during September 2004, March 2009, and April 2016. SVLFEs may be linked to the occurrence of large megathrust earthquakes. We only used onshore broadband seismograms, since seafloor observations are still limited and not common in other subduction zones. To analyze SVLFEs precisely, we used synthetic seismograms obtained via numerical simulation with a 3-D model, rather than a conventional 1-D model. Focal mechanisms and locations of SVLFEs were precisely estimated, even for those without seafloor observations. Low-angle thrust faulting solutions were concentrated around the accretionary prism toe. Our results suggest seismic slip around the very shallow part of the Philippine Sea plate boundary.

1. Introduction

In the Nankai subduction zone, southwest Japan, megathrust earthquakes occur repeatedly at intervals of approximately 100–150 years (e.g., Ando, 1975) due to subduction of the Philippine Sea plate (PHS) at a rate of 2–6 cm/year (e.g., Heki & Miyazaki, 2001; Seno et al., 1993). Recent observations have illustrated the spatial variation of slip deficits around the Nankai subduction zone (e.g., Noda et al., 2017; Yokota et al., 2016). On the basis of the slip deficit rate and friction law, tsunamigenic megathrust earthquake scenarios have been proposed (e.g., Hok et al., 2011; Hori et al., 2004). Another key study to understanding megathrust earthquakes in subduction zones is the study of slow earthquakes. Since slow earthquakes occur around the shallower or deeper limits of the rupture area of megathrust earthquakes, such activities may reflect stress accumulation around a megathrust zone (e.g., Obara & Kato, 2016; Schwartz & Rokosky, 2007). Very low frequency earthquake (VLFE) is a type of slow earthquakes with a dominant signal at periods of more than 10 s. VLFEs have been detected in the deeper parts of seismogenic zones in the Nankai (e.g., Ide & Yabe, 2014; Ito et al., 2007) and Cascadia (Ghosh et al., 2015) subduction zones.

VLFEs have also occurred at shallow depths in the Ryukyu (e.g., Ando et al., 2012), Nankai (e.g., Asano et al., 2015; Obara & Ito, 2005; Yamashita et al., 2015), Tohoku (e.g., Asano et al., 2008; Matsuzawa et al., 2015), and Costa Rica (Walter et al., 2013) subduction zones. Hereafter, shallow VLFE is referred to as SVLFE. Activity of SVLFEs may provide us with information on the frictional conditions around shallower parts of the plate boundaries (e.g., Saffer & Wallace, 2015). However, since SVLFEs occur far from onshore seismic networks,

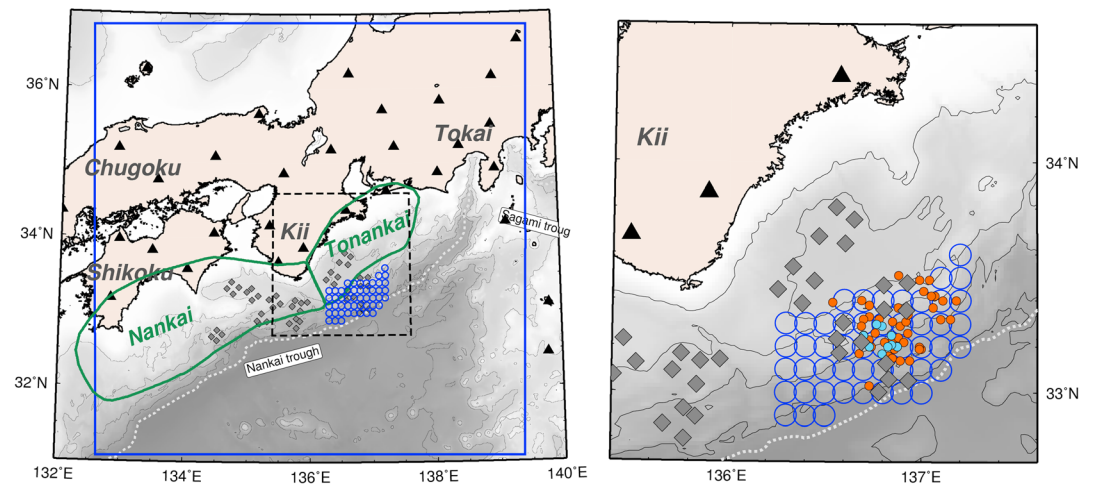


Figure 1. Map of the Nankai subduction zone, southwest Japan. Filled black triangles and gray diamonds are F-net and Dense Oceanfloor Network System for Earthquakes and Tsunamis (DONET) stations, respectively. The gray dotted line is the axis of the Nankai trough. The large blue rectangle is the horizontal coverage of region for our finite-difference method simulations. Blue open circles are assumed source grids in the moment tensor inversion. The areas enclosed by green lines represent the expected source regions of the Tonankai and Nankai earthquakes (Earthquake Research Committee, Long-term evaluation of earthquakes in the Nankai trough, 2001, available at http://www.jishin.go.jp/main/chousa/01sep_nankai/index.htm). The right panel is an enlargement of the area enclosed by the dashed line in the left panel. Orange and blue filled circles in the right panel are shallow very low frequency earthquakes that occurred in September 2004 (Ito & Obara, 2006) and March 2009 (Sugioka et al., 2012), respectively.

a conventional analysis using a one-dimensional (1-D) velocity structure is not expected to be accurate due to offshore lateral heterogeneities related to the subducting plate and accretionary prism (e.g., Takemura et al., 2016, 2018), especially since the accretionary prism has a significant influence on seismic wave propagation for periods around predominant periods of SVLFE signals (e.g., Furumura et al., 2008; Shapiro et al., 2002).

Dense Oceanfloor Network System for Earthquakes and Tsunamis (DONET; filled diamonds in Figure 1) was deployed around the Nankai trough (Kaneda et al., 2015; Kawaguchi et al., 2015). Installation of DONET stations off the southeast Kii Peninsula and off the southeast Shikoku was completed in 2011 and 2015, respectively. DONET is operated in a collaborative manner by the Japan Agency for Marine-Earth Science and Technology and National Research Institute for Earth Science and Disaster Resilience (NIED). This permanent seafloor network enables us to investigate offshore seismic activity including slow earthquakes (e.g., Annoura et al., 2017; Kaneko et al., 2018; Nakano et al., 2016, 2018; Toh et al., 2018; Wallace et al., 2016); however, the observation period of the seafloor network is still limited in comparison to onshore seismic networks, and the installation of such a network is not common in other subduction zones.

Through the developments of computer power and simulation code, centroid moment tensor (CMT) inversions of offshore earthquakes using Green's functions evaluated by numerical simulations using a regional-scale three-dimensional (3-D) velocity structure model have been conducted in some trial studies (e.g., Hejrani et al., 2017; Hingee et al., 2011; Okamoto et al., 2017; Takemura et al., 2018). The results of 3-D CMT inversions are generally better than the solutions of traditional 1-D analysis if the assumed 3-D model is suitable. The combination of a suitable 3-D model and onshore seismic network enables us to investigate long-term activity of offshore regular and slow earthquakes, including activity prior to the deployment of cabled networks or between temporal seafloor observations.

In this study, we conducted CMT inversions of SVLFEs that occurred off the southeast Kii Peninsula, Japan, using the onshore NIED broadband seismic network. A set of Green's functions was evaluated via numerical simulation of seismic wave propagation solving equations of motion in a 3-D heterogeneous subsurface structure model based on the staggered-grid finite-difference method (FDM). All CMT solutions of analyzed SVLFEs, including ones prior to seafloor observations, were characterized by low-angle thrust faulting, and these centroid locations were concentrated around the accretionary prism toe.

2. Data and Methods

In this study, we used velocity seismograms recorded at broadband F-net stations (filled triangles in Figure 1). F-net is the full-range seismograph network operated by NIED (Okada et al., 2004), and its performance is systematically monitored (Kimura et al., 2015). We validated the method for our CMT inversion using SVLFs listed in the catalog of Sugioka et al. (2012) that occurred in March 2009 and were analyzed using records of ocean bottom seismometers deployed just above the source region of the SVLFs. In the same region, Ito and Obara (2006) analyzed SVLFs that occurred in September 2004 but using onshore data and a 1-D velocity structure model. We reanalyzed these SVLFs using our 3-D model. We also conducted CMT inversions of SVLFs in April 2016, which occurred a few days after a moderate-size (M_w 5.6) interplate earthquake on 1 April 2016 (Takemura et al., 2018). SVLFs in April 2016 were visually inspected from F-net velocity seismograms for periods of 20–50 s.

A set of Green's functions was evaluated via numerical simulations based on parallel code of staggered-grid FDM for seismic wave propagation (Furumura & Chen, 2004; Takemura, Furumura, & Maeda, 2015). The simulation region of $640 \times 640 \times 192 \text{ km}^3$ (blue rectangle in Figure 1) was discretized by grid intervals of 0.25 km in the horizontal directions and 0.125 km in the vertical direction. The time interval and total number of time steps were 0.005 s and 40,000, respectively. Other technical details are the same as in Takemura, Furumura, & Maeda (2015). We employed the 3-D velocity structure model, which includes the subducting PHS, the crustal structure and bedrock topography from Koketsu et al. (2012), and a 3-D model of the accretionary prism. The 3-D structure model of the accretionary prism was constructed based on the method of Takemura, Akatsu, et al. (2015) from the simplified 1-D S wave velocity structures beneath the DONET network (Tonegawa et al., 2017), which are represented by a function proposed by Ravve and Koren (2006). Other parameters for P -wave velocity, density, and attenuation within the accretionary prism were calculated using the empirical relationships of Brocher (2005, 2008). Details of the 3-D model construction are described in Text S1 in the supporting information. A cross section of the assumed S wave velocity structure along profile A-B is shown in Figure 2a. According to the grid interval and minimum S wave velocity in the solid column, our FDM simulation can evaluate seismic wave propagation for periods longer than 8 s.

Seismic sources of five basis moment tensors except for an isotropic one (Kikuchi & Kanamori, 1991) were assumed at each source grid, which was assumed to project onto the PHS boundary at a horizontal interval of 0.1° (blue circles in Figure 1 and yellow stars in Figure 2a) and covered the epicenter region of SVLFs determined using DONET records (Nakano et al., 2016). A cosine-type moment rate function with a duration of τ s (see Figure 4d of Maeda et al., 2017) was employed. After FDM simulations, moment rate functions with $\tau = 10$ –50 s were convolved to make Green's functions with various source durations.

We conducted CMT inversions of SVLFs using Green's functions with each source grid (centroid location), duration, and centroid time. The grid interval for centroid time and source duration is 1 s. In our CMT inversions, we only selected F-net stations around the Kii, eastern Shikoku, and Chugoku area, where seismic waves pass through the region around DONET stations. We evaluated variance reductions (VRs) between observed seismograms and synthetic seismograms of each solution. The result with maximum VR is the optimal solution with moment tensor, source duration, centroid location, and time. In cases of seismograms with low signal-to-noise ratio or multiple (successive) SVLFs, we conducted CMT inversion by manually changing the centroid time to fit the initial part of observed large-amplitude surface waves. We selected the CMT solutions with VR equal to or greater than 50%.

3. Results

We obtained 46 CMT solutions of SVLFs that occurred in September 2004, March 2009, and April 2016. Estimated moment magnitudes (M_w) range from 3.5 to 4.3, and source durations range from 10 to 25 s. All solutions and waveform fittings of analyzed SVLFs are illustrated in Figures S1–S46. Estimated source parameters are listed in Data Sets S1–S3. In Figures S1–S33, we compare our CMT solutions with those listed in the catalogs by Ito and Obara (2006) and Sugioka et al. (2012).

Figure 2b shows the results of CMT inversion of an example SVLFE that occurred on 24 March 2009 (Event 2 of Table 1 in Sugioka et al., 2012). Our CMT results practically reproduced the observed onshore seismograms (right subfigure of Figure 2b). The centroid location and focal mechanism are very similar to the solution

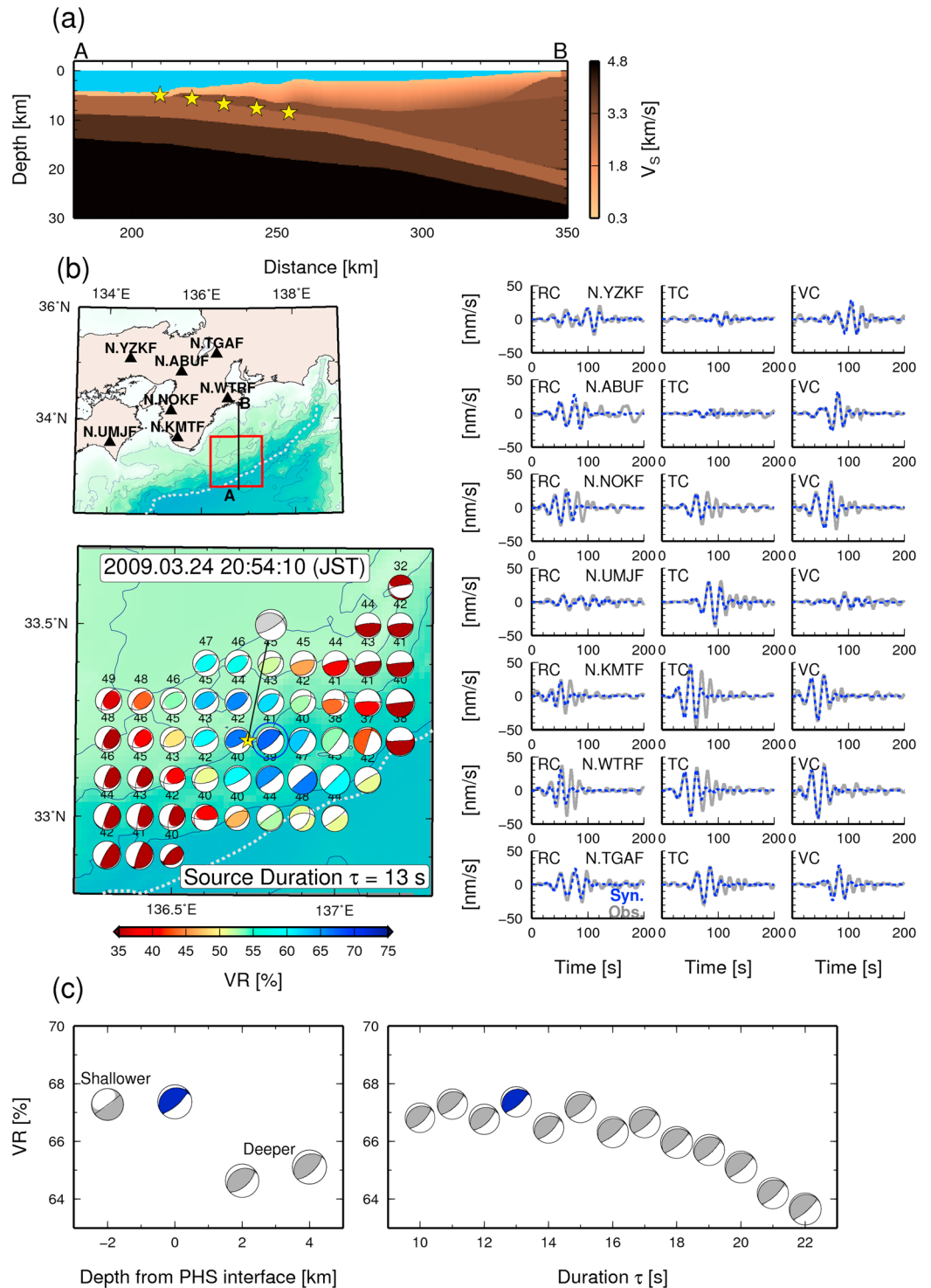


Figure 2. (a) Assumed S wave velocity structure model along profile A-B, (b) result of CMT inversion for a shallow very low frequency earthquake that occurred on 24 March 2009. (c) VRs as a function of centroid depth and duration τ . Stars in (a) are assumed source grids. The CMT solutions enclosed by the blue circle in (b) is the optimal solution and the number above each focal sphere is the centroid time delay from the time shown in the upper right side of the map, which is the origin time of Sugioka et al. (2012). The yellow star and gray focal sphere in (b) are the solution by Sugioka et al. (2012). The right subfigure of (b) shows a comparison between observed (gray line) and synthetic (dashed blue line) velocity waveforms of the optimal CMT solution for periods of 20–50 s from the estimated centroid time. In (c), other parameters except for depth or duration were fixed. The blue CMT solution represents the optimal solution. PHS = Philippine Sea plate; VR = variance reduction; CMT = centroid moment tensor.

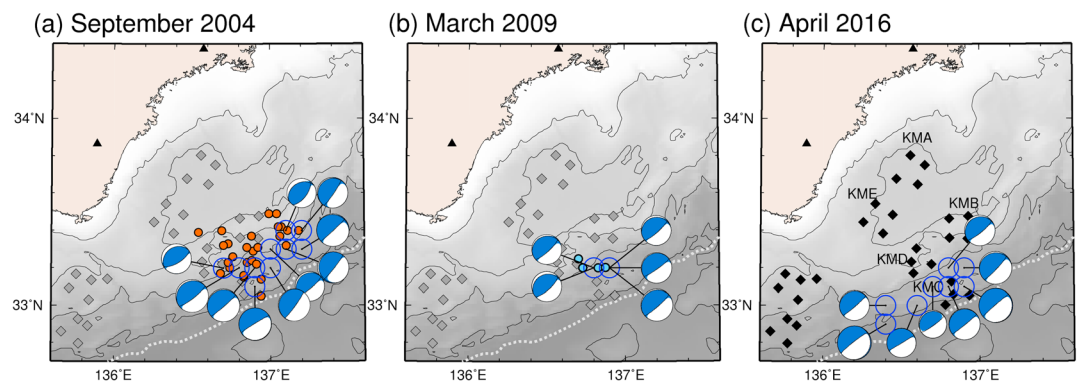


Figure 3. Spatial variations of estimated centroid moment tensor solutions of shallow very low frequency earthquakes in (a) September 2004, (b) March 2009, and (c) April 2016. Plotted focal mechanisms in (a) and (c) are solutions of the largest magnitude events at each grid. All estimated solutions are listed in Data Sets S1–S3. Filled triangles and diamonds are F-net and stations, respectively. Operated and undeveloped stations for each observation period are marked by black and gray colors, respectively. In (c), the names of DONET nodes off the southeast Kii Peninsula are represented by three capital letters. Orange circles in (a) and blue circles in (b) represent the epicenters of shallow very low frequency earthquakes referred from the catalogs of Ito and Obara (2006) and Sugioka et al. (2012), respectively.

obtained by Sugioka et al. (2012), although the estimated duration and centroid time are different. Sugioka et al. (2012) analyzed SVLFs using broadband ocean bottom seismometers, which were temporarily deployed very close to the epicenters of SVLFs. Such near-source observations can resolve the complex rupture processes of SVLFs (Sugioka et al., 2012), while our simple method using onshore seismograms and assuming a single cosine-type moment rate function cannot retrieve a detailed source rupture process. However, since synthetic seismograms using the optimal solution practically correspond to those observed at F-net stations (Figure S47), including stations unused in CMT inversion, our method captures the major characteristics of this event. We additionally synthesized Green's functions with source grinds of 2 km shallower/deeper and 4 km deeper from the PHS boundary to test the depth resolution of our method. Figure 2c shows VRs as a function of source depth and duration. The VRs do not vary significantly with depth, while deeper solutions show slightly small VRs. Some previous studies (e.g., Okamoto et al., 2017; Takemura et al., 2018) also demonstrated that precise depth estimation of offshore earthquakes via CMT inversion is difficult using only onshore long-period seismograms. We also conducted CMT inversions of other SVLFs listed in the catalog of Sugioka et al. (2012) and obtained five CMT solutions with VRs equal to or greater than 50% (Figures 3b and S29–33). These results (Figures S29–33) agree well with the solutions in Sugioka et al. (2012). Our method could not precisely identify centroid depths of SVLFs due to the lack of near-source offshore observations, but we did obtain accurate moment tensors and epicenter locations from seismograms observed at onshore broadband seismic stations only.

Figure 3a shows the spatial variations of estimated CMTs for SVLFs that occurred in September 2004, which are listed in Ito and Obara (2006). The CMT solutions with maximum M_w at each source grid were plotted. Estimated centroid times were shifted to the negative from those using the 1-D model (see Figures S1–S28) due to incorporating the 3-D model of the low-velocity accretionary prism. Centroid locations are concentrated to the south of DONET KMB and KMD nodes (locations of DONET nodes are shown in Figure 3c). Ito and Obara (2006) interpreted SVLFs as slip that occurred along the splay faults within the accretionary prism due to their relatively high-angle reverse faulting solutions estimated using the 1-D model (gray focal spheres in Figures S1–S28). However, all our CMT solutions based on the 3-D model are characterized by low-angle ($4\text{--}20^\circ$) thrust faulting (blue focal spheres in Figures S1–S28). The strike angles of estimated CMTs tend to be parallel to the trough axis. Takemura et al. (2018) demonstrated that such differences of estimated focal mechanisms between 1-D and 3-D models are mainly caused by the subducting PHS slab (see Figures 6 and 7 in their work). According to our CMT solutions, we interpret that SVLFs during September 2004 were also thrust faulting that occurred on or near the PHS boundary, the same as the SVLFs during March 2009 (Sugioka et al., 2012).

We additionally conducted CMT inversion of 13 SVLFs that occurred from 5 to 10 April 2016 (Figures S34–S46). Estimated CMT solutions are on the west of the target region and are spread along strike near the trough axis.

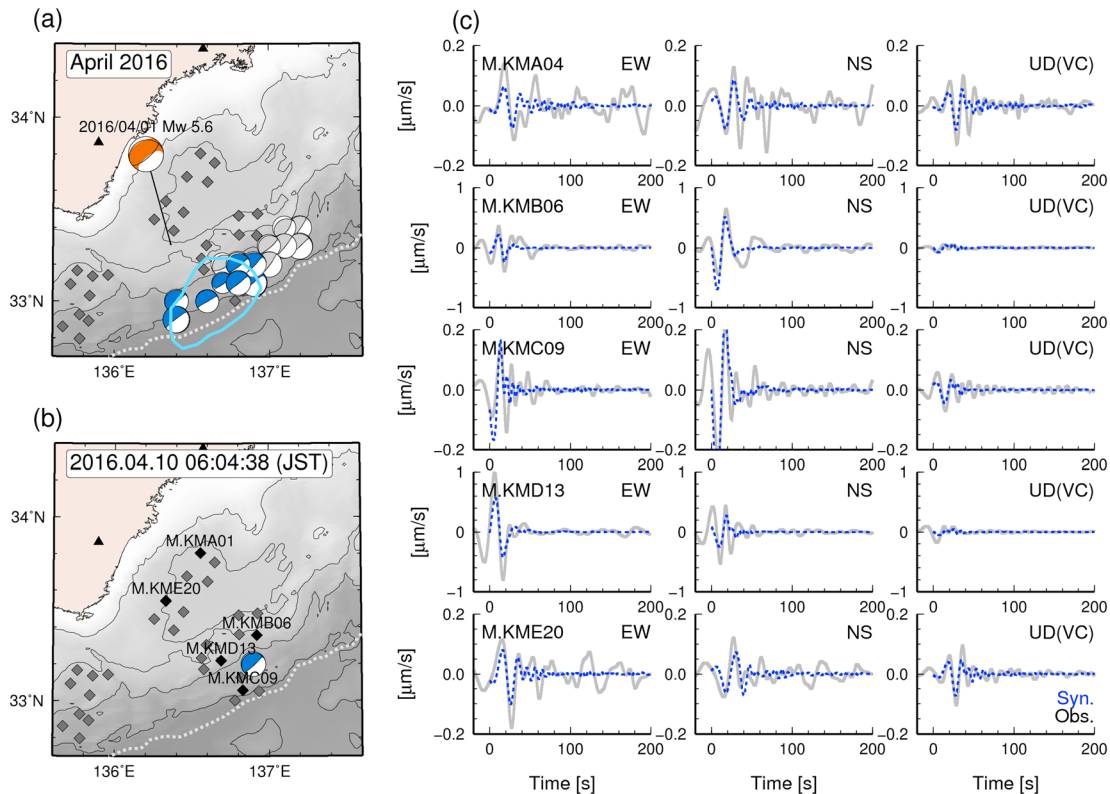


Figure 4. (a) Moment tensor solutions of shallow very low frequency earthquakes (SVLFs) from 5 to 10 April 2016. Each focal sphere is that of the event with the maximum magnitude at each grid. Gray focal spheres are solutions of SVLFs that occurred in September 2004 and March 2009. The enclosed blue area represents the epicenter area of shallow tremors detected by Annoura et al. (2017). A red focal sphere shows the centroid moment tensor solution of the 2016 Mw 5.6 regular earthquake southeast offshore Mie on 1 April 2016 (Takemura et al., 2018). (b) Map of station and hypocenter and (c) comparison of DONET velocity seismograms between observations (gray lines) and synthetics (blue lines) from the estimated centroid time. A band-pass filter with periods of 20–50 s was applied to each seismogram. Synthetic seismograms were evaluated by using Green’s functions in the 3-D model and the centroid moment tensor solution of an SVLFE occurred on 10 April 2016 (Event 13 of Data Set S3).

Centroid locations of SVLFs in April 2016 are different from previous activity (Figures 3a, 3b, and 4a) but the focal mechanisms are commonly characterized by low-angle thrust faulting, suggesting seismic slip near a very shallow part of the PHS boundary.

4. Discussion

The CMT solutions in this study, including SVLFs prior to the deployment of the seafloor seismic network, are characterized by low-angle thrust faulting mechanism and are concentrated around the accretionary prism toe. These results suggest that seismic slip occurred on or near the very shallow part of the PHS boundary, rather than within the accretionary prism (Ito & Obara, 2006). By combination of a suitable 3-D model and onshore broadband network, we confirmed that seismic slips due to SVLFs repeatedly occurred on or near the PHS boundary from 2004 to 2016.

Tonegawa et al. (2017) detected low-velocity zones at depths of approximately 5–7 km below KMB and KMD nodes. Detected low-velocity zones within the accretionary prism toes, which may be characterized by high pore fluid pressure, correlated with SVLFE activity in 2015 determined by DONET stations (Nakano et al., 2016). All CMT solutions of SVLFs analyzed in this study, including those prior to the deployment of seafloor observations in this area, are also concentrated around nodes KMB, KMC, and KMD of DONET. The occurrence of SVLFs may be related to pore fluid pressure near the PHS boundary. Our CMT inversions also revealed a spatial relationship between the occurrence of SVLFs and the slip deficit rate. The centroid locations of SVLFs are also correlated with the zone of relatively high slip deficit rate (e.g., Noda et al., 2017; Yokota et al., 2016).

We focused our attention on SVLFE activity in April 2016. Figure 4a shows the estimated CMTs of SVLFEs occurred that from 5 to 10 April 2016. The centroids of these SVLFEs are located westward in the area compared to other SVLFEs (gray focal mechanisms). High pore fluid pressure around the PHS boundary beneath this region is expected (e.g., Saffer & Wallace, 2015; Toneyawa et al., 2017). Spatial variation of structural and frictional properties on the PHS boundary is important to understanding frictional properties near the PHS boundary. Furthermore, since the region of SVLFEs could be a source of tsunamigenic earthquakes (Sugioka et al., 2012), the southwest part of our study area also has the potential to generate tsunamis. Coseismic slips at very shallow part of plate boundary can cause large sea bottom deformation and tsunamis (e.g., Maeda et al., 2011). Our CMT inversion using long-term broadband data enables us to evaluate the spatial variations of SVLFEs and find possible tsunami sources around the shallow plate boundary in future study.

The blue enclosed area in Figure 4a represents the region where low-frequency tremors occurred from 4 to 10 April 2016 (Annoura et al., 2017); centroid locations correspond well to this area. Araki et al. (2017) reported the occurrence of a slow slip event (SSE) with slip of 2–4 cm near the trough during this period. Nakano et al. (2018) reported that SVLFE activity in April 2016 correlated with SSEs. SVLFEs, low-frequency tremors, and SSE simultaneously occurred around the very shallow part of the PHS interface, near the trough axis, in April 2016.

Signals of SVLFEs in April 2016 were also recorded at DONET stations, which were not used in our CMT inversion based on onshore records. A comparison of synthetics of our CMT solutions with seismograms observed at DONET stations supports our results. Using the solution of an SVLFE occurred on 10 April 2016 (Figures 4b and S46), we synthesized the velocity seismograms at DONET stations. Figure 4c shows comparisons of velocity seismograms for periods of 20–50 s at five DONET stations. Observed seismograms were constructed by correcting the sensor orientation (Nakano et al., 2012). Although observed DONET seismograms are very noisy, especially at stations KMA04 and KME20, our synthetic seismograms correspond well to the observed ones. Large amplitude SVLFE signals appear in horizontal components at M.KMB06, M.KMC09, and M.KMD13 stations, indicating that the centroid location should be in the area enclosed by the indicated stations. If the Green's functions of shallower or deeper source grids are used (Figures S48 and S49), VRs obtained from onshore records are not different (similar to Figure 2c), but the fittings of observed DONET seismograms become worse. These comparisons validate our assumption of source grids located on the PHS boundary. Although onshore observations could not identify the centroid depth even for Green's functions of the 3-D model, near-source seafloor observations may help to overcome this problem for offshore earthquakes.

Acknowledgments

We used F-net and DONET broadband velocity seismograms, which were available from NIED website (<https://hinetwww11.bosai.go.jp/auth/?LANG=en>). The SVLFE catalog of Sugioka et al. (2012) was downloaded from the website of *Slow Earthquake Database* (Kano et al., 2018; <http://www-solid.eps.s.u-tokyo.ac.jp/~sloweq/>). We thank T. Maeda, A. Takeo, A. Noda, and S. Yabe for useful discussions. We are grateful for Y. Ito for providing the SVLFE catalog of Ito and Obara (2006). We also thank two anonymous reviewers and the Editor G. Hayes for careful reviewing and constructive comments, which have helped improve the manuscript. Generic Mapping Tools (Wessel et al., 2013) and Seismic Analysis Code (SAC; Helffrich et al., 2013) were used to create figures and conduct signal processing, respectively. FDM simulations were conducted on the Earth Simulator of the JAMSTEC. Bathymetric depth data were obtained from ETOPO1 (Amante & Eakins, 2009; <http://www.ngdc.noaa.gov/mgg/global/global.html>). The 3-D layered structure of the JIVSM (Koketsu et al., 2012) is available via the Japanese website (http://www.jishin.go.jp/main/chousa/12_choshuki/dat/). This study was supported by the Grants-in-Aid program of the Japan Society for the Promotion of Science (17K14382).

References

- Amante, C., & Eakins, B. W. (2009). ETOPO1 1 Arc-Minute Global Relief Model: Procedures, Data Sources and Analysis. NOAA Technical Memorandum NESDIS NGDC-24. National Geophysical Data Center, NOAA. <https://doi.org/10.7289/V5C8276M>
- Ando, M. (1975). Source mechanism and tectonic significance of historical earthquakes along the Nankai Trough, Japan. *Tectonophysics*, 27(2), 119–140. [https://doi.org/10.1016/0040-1951\(75\)90102-X](https://doi.org/10.1016/0040-1951(75)90102-X)
- Ando, M., Tu, Y., Kumagai, H., Yamashita, Y., & Lin, C.-H. (2012). Very low-frequency earthquakes along the Ryukyu subduction zone. *Geophysical Research Letters*, 39, L04303. <https://doi.org/10.1029/2011GL050559>
- Annoura, S., Hashimoto, T., Kamaya, N., & Katsumata, A. (2017). Shallow episodic tremor near the Nankai Trough axis off southeast Mie prefecture, Japan. *Geophysical Research Letters*, 44, 3564–3571. <https://doi.org/10.1002/2017GL073006>
- Araki, E., Saffer, D. M., Kopf, A. J., Wallace, L. M., Kimura, T., Machida, Y., et al. (2017). Recurring and triggered slow-slip events near the trench at the Nankai Trough subduction megathrust. *Science*, 356, 1157. <https://doi.org/10.1126/science.aan3120>
- Asano, Y., Obara, K., & Ito, Y. (2008). Spatiotemporal distribution of very-low frequency earthquakes in Tokachi-oki near the junction of the Kuril and Japan trenches revealed by using array signal processing. *Earth, Planets and Space*, 60, 871–875.
- Brocher, T. M. (2005). Empirical relations between elastic wave-speeds and density in the Earth's crust. *Bulletin of the Seismological Society of America*, 95(6), 2081–2092. <https://doi.org/10.1785/0120050077>
- Brocher, T. M. (2008). Key elements of regional seismic velocity models for long period ground motion simulations. *Journal of Seismology*, 12(2), 217–221. <https://doi.org/10.1007/s10950-007-9061-3>
- Furumura, T., & Chen, L. (2004). Large scale parallel simulation and visualization of 3D seismic wavefield using Earth simulator. *Computer Modeling in Engineering and Sciences*, 6, 153–168. <https://doi.org/10.3970/cmescs.2004.006.153>
- Furumura, T., Hayakawa, T., Nakamura, M., Koketsu, K., & Baba, T. (2008). Development of long-period ground motions from the Nankai Trough, Japan, earthquake: Observations and computer simulation of the 1944 Tonankai (Mw 8.1) and the 2004 SE Off-Kii Peninsula (Mw 7.4) earthquakes. *Pure and Applied Geophysics*, 165(3–4), 585–607. <https://doi.org/10.1007/s00024-008-0318-8>
- Ghosh, A., Huesca-Pérez, E., Brodsky, E., & Ito, Y. (2015). Very low-frequency earthquakes in Cascadia migrate with tremor. *Geophysical Research Letters*, 42, 3228–3232. <https://doi.org/10.1002/2015GL063286>
- Hejrani, B., Tkalčić, H., & Fichtner, A. (2017). Centroid moment tensor catalogue using a 3-D continental scale Earth model: Application to earthquakes in Papua New Guinea and the Solomon Islands. *Journal of Geophysical Research: Solid Earth*, 122, 5517–5543. <https://doi.org/10.1002/2017JB014230>
- Heki, K., & Miyazaki, S. (2001). Plate convergence and long-term crustal deformation in central Japan. *Geophysical Research Letters*, 28(12), 2313–2316. <https://doi.org/10.1029/2000GL012537>

- Helfrich, G., Wookey, J., & Bastow, I. (2013). *The seismic analysis code: A primer and user's guide*. Cambridge: Cambridge University Press. <https://doi.org/10.1017/CBO9781139547260>
- Hingee, M., Tkalčić, H., Fichtner, A., & Sambridge, M. (2011). Seismic moment tensor inversion using a 3-D structural mode: Applications for the Australian region. *Geophysical Journal International*, 184(2), 949–964. <https://doi.org/10.1111/j.1365-246X.2010.04897.x>
- Hok, S., Fukuyama, E., & Hashimoto, C. (2011). Dynamic rupture scenarios of anticipated Nankai-Tonankai earthquakes, southwest Japan. *Journal of Geophysical Research*, 116, B12319. <https://doi.org/10.1029/2111JB008492>
- Hori, T., Kato, N., Hirahara, K., Baba, T., & Kaneda, Y. (2004). A numerical simulation of earthquake cycle along the Nankai Trough in southwest Japan: Lateral variation in frictional property due to the slab geometry controls the nucleation position. *Earth and Planetary Science Letters*, 228(3–4), 215–226. <https://doi.org/10.1016/j.epsl.2004.09.033>
- Ide, S., & Yabe, S. (2014). Universality of slow earthquakes in the very low frequency earthquakes in the very low frequency band. *Geophysical Research Letters*, 41, 2786–2793. <https://doi.org/10.1002/2014GL059712>
- Ito, Y., & Obara, K. (2006). Dynamic deformation of the accretionary prism excites very low frequency earthquakes. *Geophysical Research Letters*, 33, L02311. <https://doi.org/10.1029/2005GL025270>
- Ito, Y., Obara, K., Shiomi, K., Sekine, S., & Hirose, H. (2007). Slow earthquakes coincident with episodic tremors and slow slip events. *Science*, 315(5811), 503–506. <https://doi.org/10.1126/science.1134454>
- Kaneko, L., Ide, S., & Nakano, M. (2018). Slow earthquakes in the microseism frequency band (0.1–1.0 Hz) off Kii Peninsula, Japan. *Geophysical Research Letters*, 45, 2618–2624. <https://doi.org/10.1002/2017GL076773>
- Kano, M., Aso, N., Matsuzawa, T., Ide, S., Annoura, S., Arai, R., et al. (2018). Development of a slow earthquake database. *Seismological Research Letters*: <https://doi.org/10.1785/0220180021>, 89(4), 1566–1575.
- Kaneda, Y., Kawaguchi, K., Araki, E., Matsumoto, H., Nakamura, T., Kamiya, S., et al. (2015). Development and application of an advanced ocean floor network system for megathrust earthquakes and tsunamis. In *Seafloor observatories* (pp. 643–662). Springer Praxis Books. https://doi.org/10.1007/978-3-642-11374-1_25
- Kikuchi, M., & Kanamori, H. (1991). Inversion of complex body waves-III. *Bulletin of the Seismological Society of America*, 81, 2335–2350.
- Kimura, T., Murakami, H., & Matsumoto, T. (2015). Systematic monitoring of instrumentation health in high-density broadband seismic networks. *Earth, Planets and Space*, 67(1). <https://doi.org/10.1186/s40623-015-0226-y>
- Koketsu, K., Miyake, H., & Suzuki, H. (2012). Japan integrated velocity structure model version 1. In: *Proceedings of the 15th World Conference on Earthquake Engineering*, Lisbon, Portugal, 24–28 September.
- Maeda, T., Furumura, T., Sakai, S., & Shinohara, M. (2011). Significant tsunami observed at ocean-bottom pressure gauges during the 2011 off the Pacific coast of Tohoku earthquake. *Earth, Planets and Space*, 63(7), 803–808. <https://doi.org/10.5047/eps.2011.06.005>
- Maeda, T., Takemura, S., & Furumura, T. (2017). OpenSWPC: An open-source parallel simulation code for modeling seismic wave propagation in 3D heterogeneous viscoelastic media. *Earth, Planets and Space*, 69(1), 102. <https://doi.org/10.1186/s40623-017-0687-2>
- Matsuzawa, T., Asano, Y., & Obara, K. (2015). Very low frequency earthquakes off the Pacific coast of Tohoku, Japan. *Geophysical Research Letters*, 42, 4318–4325. <https://doi.org/10.1002/2015GL063959>
- Nakano, M., Hori, T., Araki, E., Kodaira, S., & Ide, S. (2018). Shallow very-low-frequency earthquakes accompany slow slip events in the Nankai subduction zone. *Nature Communications*, 9(1), 984. <https://doi.org/10.1038/s41467-018-03431-5>
- Nakano, M., Hori, T., Araki, E., Takahashi, N., & Kodaira, S. (2016). Ocean floor networks capture low-frequency earthquake event. *Eos*, 97. <https://doi.org/10.1029/2016EO052877>
- Nakano, M., Tonegawa, T., & Kaneda, Y. (2012). Orientations of DONET seismometers estimated from seismic waveforms. *Japan Agency for Marine-Earth Science and Technology Report of Research and Development*, 15, 77–89. <https://doi.org/10.5918/jamstecr.15.77>
- Noda, A., Saito, T., & Fukuyama, E. (2017). Slip-deficit rate distribution along the Nankai trough, southwest Japan, with elastic lithosphere and viscoelastic asthenosphere, in the abstracts of AGU fall meeting, G52A-08
- Obara, K., & Ito, Y. (2005). Very low frequency earthquakes excited by the 2004 off the Kii Peninsula earthquakes: A dynamic deformation process in the large accretionary prism. *Earth, Planets and Space*, 57(4), 321–326. <https://doi.org/10.1186/BF03352570>
- Obara, K., & Kato, A. (2016). Connecting slow earthquakes to huge earthquakes. *Science*, 353(6296), 253–257. <https://doi.org/10.1126/science.aaf1512>
- Okada, Y., Kasahara, K., Hori, S., Obara, K., Sekiguchi, S., Fujiwara, H., & Yamamoto, A. (2004). Recent progress of seismic observation networks in Japan-Hi-net, F-net, K-NET and KiK-net. *Earth, Planets and Space*, 56(8), xv–xxviii. <https://doi.org/10.1186/BF03353076>
- Okamoto, T., Takenaka, H., Nakamura, T., & Hara, T. (2017). FFD simulation of earthquakes off western Kyushu, Japan, using a land-ocean unified 3D structure model. *Earth, Planets and Space*, 69, 88. <https://doi.org/10.1186/s40623-017-0672-9>
- Ravve, I., & Koren, Z. (2006). Exponential asymptotically bounded velocity model: Part I—Effective models and velocity transformations. *Geophysics*, 71(3), T53–T65. <https://doi.org/10.1190/1.2196033>
- Saffer, D. M., & Wallace, L. M. (2015). The frictional, hydrologic, metamorphic and thermal habitat of shallow slow earthquakes. *Nature Geoscience*, 8(3), 161–600. <https://doi.org/10.1038/NGEO2390>
- Schwartz, S., & Rokosky, J. M. (2007). Slow slip events and seismic tremor at Circum-Pacific subduction zones. *Reviews of Geophysics*, 45, RG3004. <https://doi.org/10.1029/2006RG000208>
- Seno, T., Stein, S., & Gripp, A. E. (1993). A model for the motion of the Philippine Sea plate consistent with NUVEL-1 and geophysical data. *Journal of Geophysical Research*, 98(B10), 17941–17948. <https://doi.org/10.1029/93JB00782>
- Shapiro, N. M., Olsen, K. B., & Singh, K. (2002). On the duration of seismic incident onto the Valley of Mexico for subduction zone earthquake. *Geophysical Journal International*, 151(2), 501–510. <https://doi.org/10.1046/j.1365-246X.2002.01789.x>
- Sugioka, H., Okamoto, T., Nakamura, T., Ishihara, Y., Ito, A., Obara, K., et al. (2012). Tsunamigenic potential of the shallow subduction plate boundary inferred from slow seismic slip. *Nature Geoscience*, 5(6), 414–418. <https://doi.org/10.1038/ngeo1466>
- Takemura, S., Akatsu, M., Masuda, K., Kajikawa, K., & Yoshimoto, K. (2015). Long-period ground motions in a laterally inhomogeneous large sedimentary basin: Observations and model simulations of long-period surface waves in the northern Kanto Basin, Japan. *Earth, Planets and Space*, 67(1), 33. <https://doi.org/10.1186/s40623-015-0201-7>
- Takemura, S., Furumura, T., & Maeda, T. (2015). Scattering of high-frequency wavefield caused by irregular surface topography and small-scale velocity inhomogeneity. *Geophysical Journal International*, 201(1), 459–474. <https://doi.org/10.1093/gji/ggv038>
- Takemura, S., Kimura, T., Shiomi, K., Kubo, H., & Saito, T. (2018). Moment tensor inversion of the 2016 southeast offshore Mie earthquake in the Tonankai region using a three-dimensional velocity structure model: Effects of the accretionary prism and subducting oceanic plate. *Earth, Planets and Space*, 70(1), 50. <https://doi.org/10.1186/s40623-018-0819-3>
- Takemura, S., Shiomi, K., Kimura, T., & Saito, T. (2016). Systematic difference between first-motion and waveform-inversion solutions for shallow offshore earthquakes due to a low-angle dipping slab. *Earth, Planets and Space*, 68(1), 149. <https://doi.org/10.1186/s40623-016-0527-9>

- Toh, A., Obana, K., & Araki, E. (2018). Distribution of very low frequency earthquakes in the Nankai accretionary prism influenced by a subducting-ridge. *Earth and Planetary Science Letters*, *482*, 342–356. <https://doi.org/10.1016/j.epsl.2017.10.062>
- Tonegawa, T., Araki, E., Kimura, T., Nakamura, T., Nakano, M., & Suzuki, K. (2017). Sporadic low-velocity volumes spatially correlate with shallow very low frequency earthquake clusters. *Nature Communications*, *8*(1), 2048. <https://doi.org/10.1038/s41467-017-02276-8>
- Wallace, L. M., Araki, E., Saffer, D., Wang, X., Roesner, A., Kopf, A., et al. (2016). Near-field observations of an offshore Mw 6.0 earthquake from an integrated seafloor and subseafloor monitoring network at the Nankai Trough, southwest Japan. *Journal of Geophysical Research: Solid Earth*, *121*, 8338–8351. <https://doi.org/10.1002/2016JB013417>
- Walter, J. L., Schwartz, S. Y., Protti, M., & Gonzalez, V. (2013). The synchronous occurrence of shallow tremor and very low frequency earthquakes offshore of the Nicoya Peninsula, Costa Rica. *Geophysics Research Letters*, *40*, 1517–1522. <https://doi.org/10.1002/grl.50213>
- Wessel, P., Smith, W. H. F., Scharroo, R., Luis, J., & Wobbe, F. (2013). Generic Mapping Tools: Improved version released. *Eos*, *94*(45), 409–410. <https://doi.org/10.1002/2013EO450001>
- Yamashita, Y., Yakiwara, H., Asano, Y., Shimizu, H., Uchida, K., Hirano, S., et al. (2015). Migrating tremor off southern Kyushu as evidence for slow slip of a shallow subduction interface. *Science*, *348*(6235), 676–679. <https://doi.org/10.1126/science.aaa4242>
- Yokota, Y., Ishikawa, T., Watanabe, S., Tashiro, T., & Asada, A. (2016). Seafloor geodetic constraints on interplate coupling of the Nankai Trough megathrust zone. *Nature*, *534*(7607), 374–377. <https://doi.org/10.1038/nature17632>